JSCE Journal of Earthquake Engineering

SHEAR BAND DEVELOPMENT LENGTH AND IMPLICATIONS FOR RUPTURE PROPAGATION THROUGH SOIL

Jörgen JOHANSSON[1] and Kazuo KONAGAI[2]

[1]Research Associate, Institute of Industrial Science, University of Tokyo,
Tokyo 153-8505, Japan, jorgen@iis.u-tokyo.ac.jp
[2]Professor, Institute of Industrial Science, University of Tokyo,
Tokyo 153-8505, Japan, konagai@iis.u-tokyo.ac.jp

Model experiments of reverse fault rupture propagation through sand under 1-g conditions show that he D/H ratio for the same model height (40 cm) depends on the fault dip-angle, with the largest uplift is needed for a 60 dip-angle. This is explained with a simple elastic analysis together with the concept of a characteristic shear band development length, which is estimated from model experiments considering a constant peak to residual displacement along the shear band in biaxial tests. Soil anisotropy is also a contributing factor.

Key Words: Peak to residual stress drop, shear band displacement, fault surface rupture experiment.

1. INTRODUCTION

The recent earthquakes in Turkey and Taiwan 1999, and Niigata Chuetsu, Japan, 2004 have raised the awareness of the dangers posed by tectonic fault rupture propagation up through soft soil deposits (quaternary) and the induced permanent ground deformation's effects on infrastructure below and above the ground. For design purposes there is a need for simple formulas for estimating bedrock fault offset required for surface rupture to occur; The first step to develop one such simple formula is taken here.

Most fracture mechanics studies on geomaterials have focused on saturated clays.[1–3] For sand and gravels there are many studies on shear band propagation.[4–7] The main focus of the experimental and analytical studies is on how the current stress state and material parameters affects the initiation and inclinations of the shear bands in element tests since these two factors changes the load-deformation curves, on which soil's stress-strain behavior is based; To obtain mesh independent solutions to geotechnical boundary value problems are also important (see e.g. Wang et. al.[8]).

Important parameters such as 1) the amount of bedrock uplift necessary for a surface rupture to occur and 2) approximately where on the ground surface it will appear and their relation to material parameters such as dilatancy and friction angle have been investigated with model experiments such as trap-door experiments e.g.,[9] long shear-box experiments,[10] and fault rupture experiments.[11–16]

Scarpelli and Wood[10] and Stone and Wood[12] also estimated the shear band development length by measuring dilation at different locations along the shear band. The shear band development length[17] (end region,[1] shear band tip,[9] and tip length[10] are other names are available in the literature) is defined as the distance from the shear band tip which is assumed to be at peak state to a point further behind on the shear band which is at residual state (see also Fig. 3.) The shear band development length together with the stress drop from peak to residual state play an important roll in the progressive failure of geomaterials (see Puzrin and Germanovich[18] for one application). Muir-Wood[5] points out that information shear band development lengths are sparse in the literature.

We attempt to estimate characteristic shear band lengths from the above mentioned rupture model experiments based on observations in biaxial tests that the displacement along a shear band, needed for the load to go from peak to residual level, is parameter depending mainly on the sand's mean grain size, D_{50}.[19] We analyze and discuss the results of a few researchers, and try to explain scale effects observed and not observed in some of the model rupture experiments.

2. METHOD

Yoshida et. al.[19] observed in biaxial tests on several sands and gravels, that the relative displacement, D_{PR}, between the two sides along a shear band needed for the load to go from peak to residual level (see schematic Figure 1), depends mainly

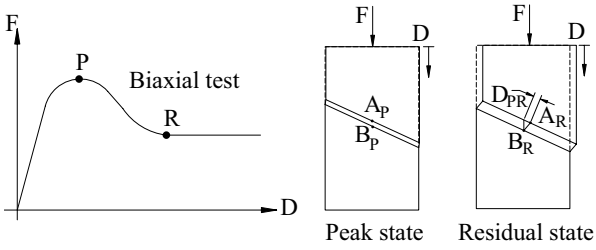

Figure 1: Schematic explanation of relative displacement along the shear band, D_{pr} for the load to go from peak to residual level in a biaxial test.

on the mean grain size as

$$D_{PR} = 6.52 {D_{50}}^{0.69} \quad (1)$$

(see Figure 2 , observe: D_{50}must be in mm.). Equation 1 is based on data from Yoshida and Tatsuoka;[19] Recently Oie et. al.[7] presented similar regression curves, now also for well-graded soils, and concluded that the $D_{PR}$is independent of confining pressure for the range in their tests.

Palmer and Rice[1] derives an explicit formula for relation between the shear band development length, L_d, and the shear displacement, D_{PR}, (called ω and δ Palmer and Rice[1]) and the shear stress drop $\Delta\tau = \tau_{\text{peak}} - \tau_{\text{residual}}$. Therefore, in addition to the shear band length scale effect pointed by Bishop,[17] there is another scale effect for frictional materials since the stress drop,

$$\Delta\tau = \sigma_{normal}(\tan\phi_{\text{peak}} - \tan\phi_{\text{residual}}),$$

is dependent on the failure surface normal pressure, which changes with e.g. overburden pressure.

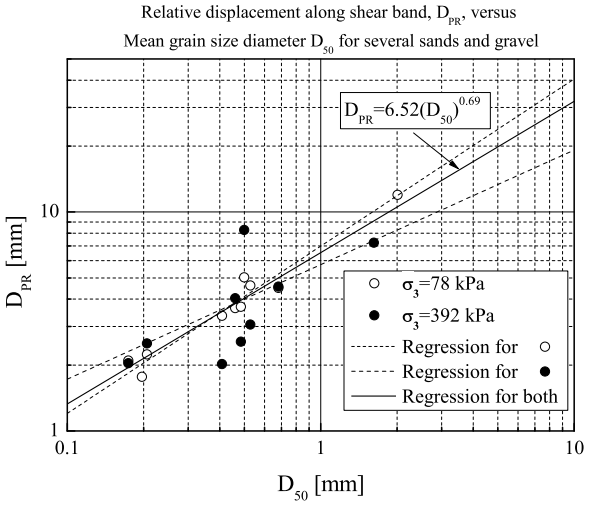

Figure 2: Relative displacement along the shear band, D_{pr} versus mean grain size diameter, D_{50}(partially after.[19])

The stress conditions does of course not only change with overburden pressure but also changes with change of loading conditions during the progressive failure. For shear band/rupture propagation through soil due to a dip-slip reverse fault bedrock dislocation, the horizontal normal stresses increases simultaneously as the shear band propagates toward the surface, thus the shear band development length changes during the course of the rupture. To simplify the problem we assume there exist a *characteristic* shear band development length, L_d along the rupture, which can be considered an average of the actual shear band development length along the whole shear band.

We assume that for a displacement, D_{PR}, in the direction of the shear band at the base of the soil deposit, the shear band propagate a distance L_d as shown in Figure 3 a). The tip of the shear band, point P, is at peak state while point R is at residual state. Points in between P and R are on their way to residual state. Points below the top most R are all in residual state. After an additional displacement $D_{PR}$of the base, the total displacement is now $2D_{PR}$. Point A which was at distance $D_{pr}$from the peak state point, P, in Figure 3 a) has moved a distance of D_{PR} and reached A' in Figure 3 b) and now this location is at residual state (marked R) and the shear band has propagated another L_d. Continuing like this we can add n displacements , D_{PR}, and set this equal the displacement necessary for a surface

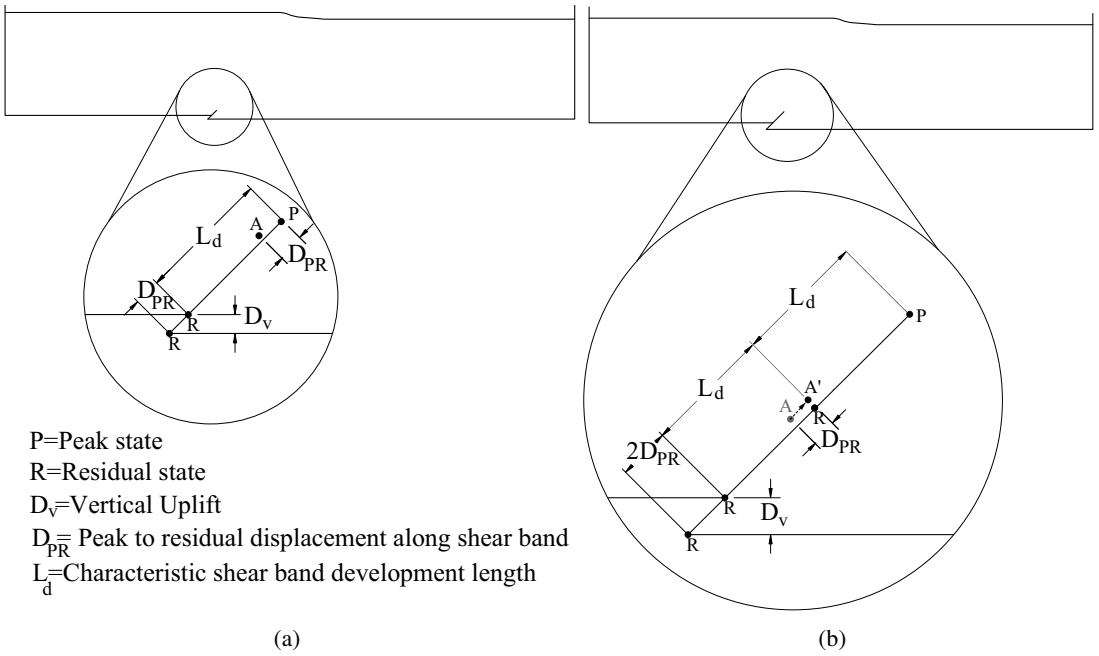

Figure 3: Explanation of simplified shear band propagation approach. Each displacement along the shear band, $\mathrm{D_{pr}}$, will cause the shear band to propagate a distance $\mathrm{L_d}$. The tip of the shear band, Point P, is at peak state while point R is at residual state. Points in between P and R are on their way to residual state. Points behind the R are all in residual state.

rupture to occur, i.e.

$$\mathrm{D_{SR}} = n\mathrm{D_{PR}}. \tag{2}$$

Similarly we add n shear band development lengths, $\mathrm{L_d}$, and set this equal to the rupture length, $\mathrm{L_r}$, which can be approximated as shown in Figure 4. Thus we end up with

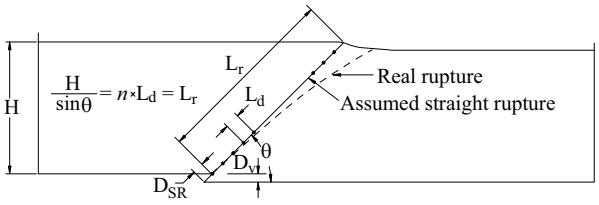

Figure 4: n relative displacements along the shear band, $\mathrm{D_{pr}}$, will make the shear band propagate to the surface. For simplicity we assume the rupture to be a straight line.

$$\mathrm{L_r} = n\mathrm{L_d} = \frac{\mathrm{H}}{\sin\theta}. \tag{3}$$

With the displacement required for a surface rupture, $\mathrm{D_{SR}}$, obtained from the experiments and estimating $\mathrm{D_{PR}}$ from Figure 2 we can compute n from equation 2. The dip-angle, θ, is given in the experiment and therefore we can compute $\mathrm{L_d}$ with equation 3.

For the analysis of Stone and Wood's results and the ones of Vardoulakis et. al. we assume that $n\mathrm{D_{PR}}$ is equal to the total uplift necessary to induce a rupture, of length $\mathrm{L_r}$, which does not reach the ground surface.

3. ANALYSIS AND PRELIMINARY RESULTS

In this preliminary study we have selected results from 4 different rupture studies.[13,15,12,9] For Tani et. al. and Lee et. al studies we have obtained vertical base offset required for surface rupture. Thus we can estimate the rupture length, $\mathrm{L_r}$, according to the deposit height as shown in Figure 4 and equation 3. For Stone et. al. and Vardoulakis we had to measure rupture lengths in their figures and the base offset normalized by the rupture length was plotted instead of normalized by height as for Tani et. al and Lee et. al. results (see Figure 5.)

Using equation 1 we estimated the relative shear band displacement, $\mathrm{D_{PR}}$as shown in Table 1 and the estimated shear band development lengths are given Figure 6 versus overburden pressure, which was computed at the middle depth of the rupture.

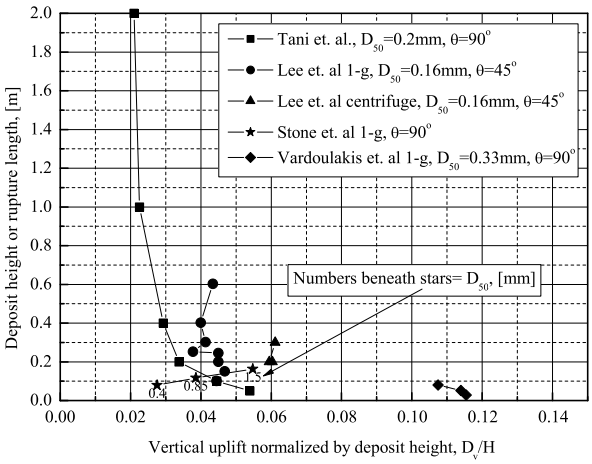

Figure 5: Height of deposit versus H versus normalized vertical uplift, D_v/H. For Stone et. al. and Vardoulakis et al. the rupture length, $L_r$versus normalized vertical uplift, $D_v/L_r$is plotted.

Table 1: Relative shear band displacement for different sands estimated with equation 1.

Researchers	Material	D_{50}[mm]	D_{pr}[mm]
Tani et. al.[13]	Toyoura sand	0.17	1.9
Lee et. al.[15]	Silica sand no.7	0.16	1.8
Stone et. al.[12]	Silver	1.5	8.6
	Leighton	0.85	5.8
	Buzzard sand	0.4	3.5
Vardoulakis et. al.[9]	Karlsruhe medium grained sand	0.33	3.0

(1) Scale effect in vertical dip-slip fault model experiment

As seen in Figure 6 Tani-Ueta's results give a shear band development length increasing with vertical overburden pressure. Since these results are for 90° dip-angle dip-slip faults, we assume there are only a minor increase in the horizontal stress due to the dilation of the material. The dilation is on the order of the mean grain size, D_{50},[19] for confining pressures of 50 kPa. For lower pressures the dilation is more,[15] but it should still be much less than the shear band thickness which is on the order of $10D_{50}$, thus 1.5 mm horizontal dilation compared to the model experiment box 1.5m gives 0.1 % over all horizontal normal strain. This is relatively small compared to the horizontal deformation of up to 20 mm for 45° dip-angle reverse faults.[15] We therefore assume the increase in horizontal confining pressure to be small and the observed increase in shear band development length is due to the increasing overburden pressure.

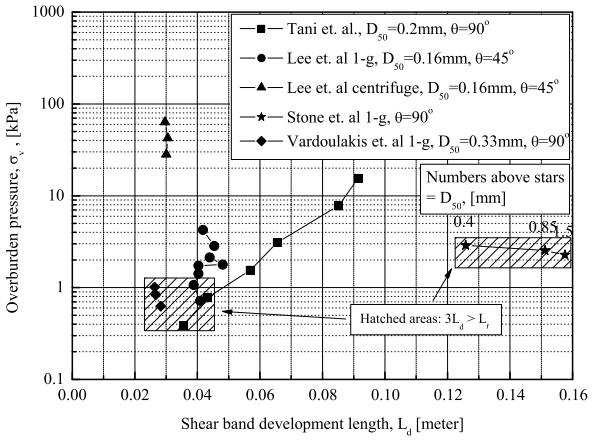

Figure 6: Confining pressure, $\sigma_v = \rho g H$ versus shear band development length, L_d. θ is the fault dip-angle.

(2) Dip-angle dependency of required uplift for surface rupture

Tani et. al. and Ueta et. al.[13,14] have observed a dip-angle dependency (for dip-slip faults) for the required uplift normalized with the deposit height for a surface rupture to occur. For the same model height (40 cm) the largest D/H ratio is needed for a 60° dip-angle reverse fault (see Figure 7 .) Normal faults (extensional faults, $\theta > 90$ in Figure 7) requires the smaller D/H ratio for a surface rupture to occur with slight increase in D/H the more horizontal the dip. We will try to explain peak in D/H

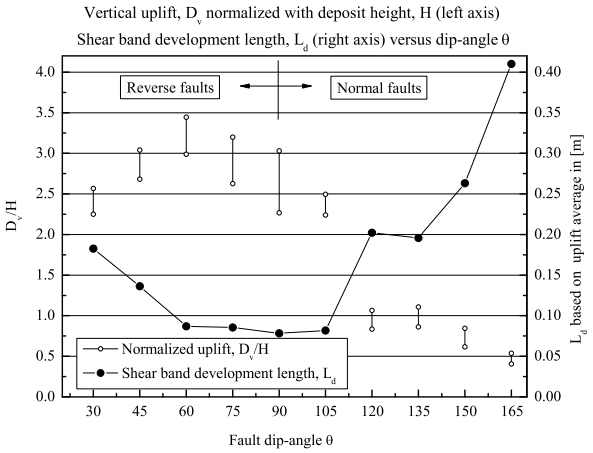

Figure 7: Vertical uplift normalized with deposit height , D_v/H versus dip-angle θ (after Tani et. al.[13])

for reverse faults with 1) anisotropic strength of soil and 2) with the help of simple elastic analysis.

Anisotropy as contributing factor Park and Tatsuoka[20] have investigated inherent anisotropy of Toyoura sand in biaxial tests. Prismatic samples with different angles between the direction of major principal stress and bedding plane were prepared by pluviating sand into a mold which could be mounted in several different angles. Figure 8

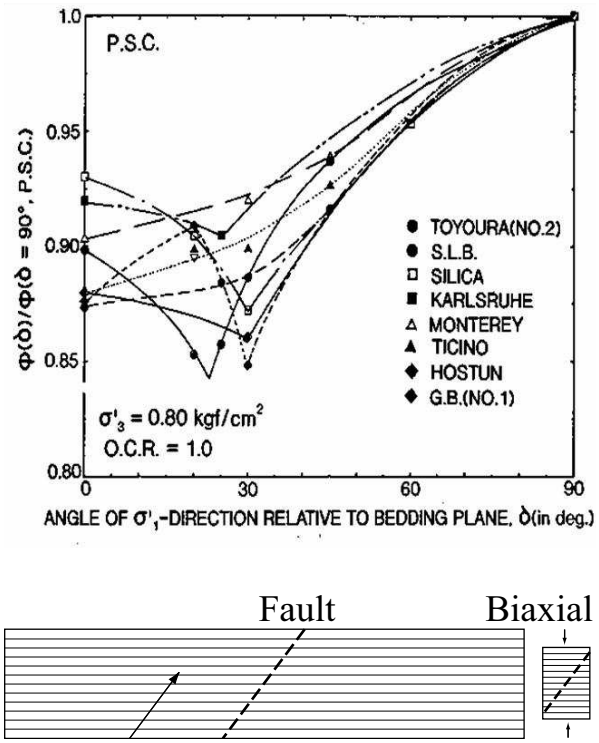

Figure 8: Friction angle versus bedding plane (after Park and Tatsuoka,[20]) as explanation for largest vertical uplift normalized with deposit height , D_v/H is needed for dip-angle θ of 60° (according to Tani et. al.[13])

shows the peak friction angle dependency on the angle between the bedding plane and the major principal stress. A minimum friction angle is obtained for bedding angle of 25 to 30° which corresponds to shear band parallel to the bedding plane. A shear band crossing the bedding planes perpendicularly would assumingly give the peak friction with in terms of inherent anisotropy, but as is known[21] two conjugate shear bands will develop and the biggest angle between the bedding plane and the conjugate shear bands is obtained for samples with bedding plane perpendicular to the major principal stress axis.

Why the minimum friction angle is obtained for a shear band parallel to the bedding plane is hypothesized on as follows. If we pour sand grains on a fairly flat surface the grains accommodate in such a way that, when under pressure, the easiest way for them to move is perpendicular to the bedding plane. This may also be an explanation for why the Young's modulus parallel to the bedding plane is larger than the one perpendicular to the bedding plane and why the Poisson ratio relating deformation perpendicular to the bedding plane to loading parallel to bedding plane is larger.[22]

For a 60° dip-angle fault the angle between the rupture plane and the bedding plane is similar to the ones observed for the peak friction angle in biaxial tests,[20] thus this may be considered to be the strongest failure plane and a contributing factor to the largest uplift necessary for surface rupture is observed for dip-angle of 60°.

Simple elastic analysis We consider the elastic deformations due to a fault of arbitrary dip-angle to be linear combination of a completely horizontal fault (0°dip-angle) and vertical fault (90°dip-angle) (personal communication[23]), thus it is sufficient to perform 2 linear elastic plane strain FE analyses.

The geometry was the same as in the experiment, a 1550 mm long box with a 400 mm thick deposit with Young's modulus, E=20 MPa, Poisson ratio, $\nu = 0.3$ and the mesh size was 25 mm (see Figure 9.) Analysis with smooth and rough

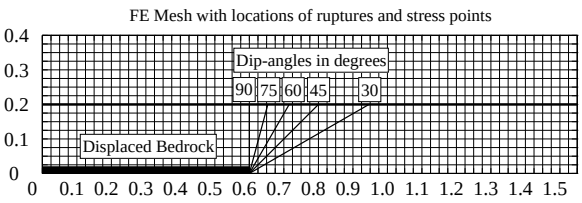

Figure 9: FE mesh with location of "ruptures" and points at which stresses and stress ratios were computed.

boundaries were performed. Setting the vertical uplift to height, D_v/H ratio to a constant for all dip-angles, i.e. the ratio of displacement along the rupture and the rupture length, D_R/L_R is equal for all dip-angles if we assume straight rupture plane as in Figure 9. The initial stresses corresponding to $K_0 = \sigma_h/\sigma_v$values of 0.5 and 0.3 were added

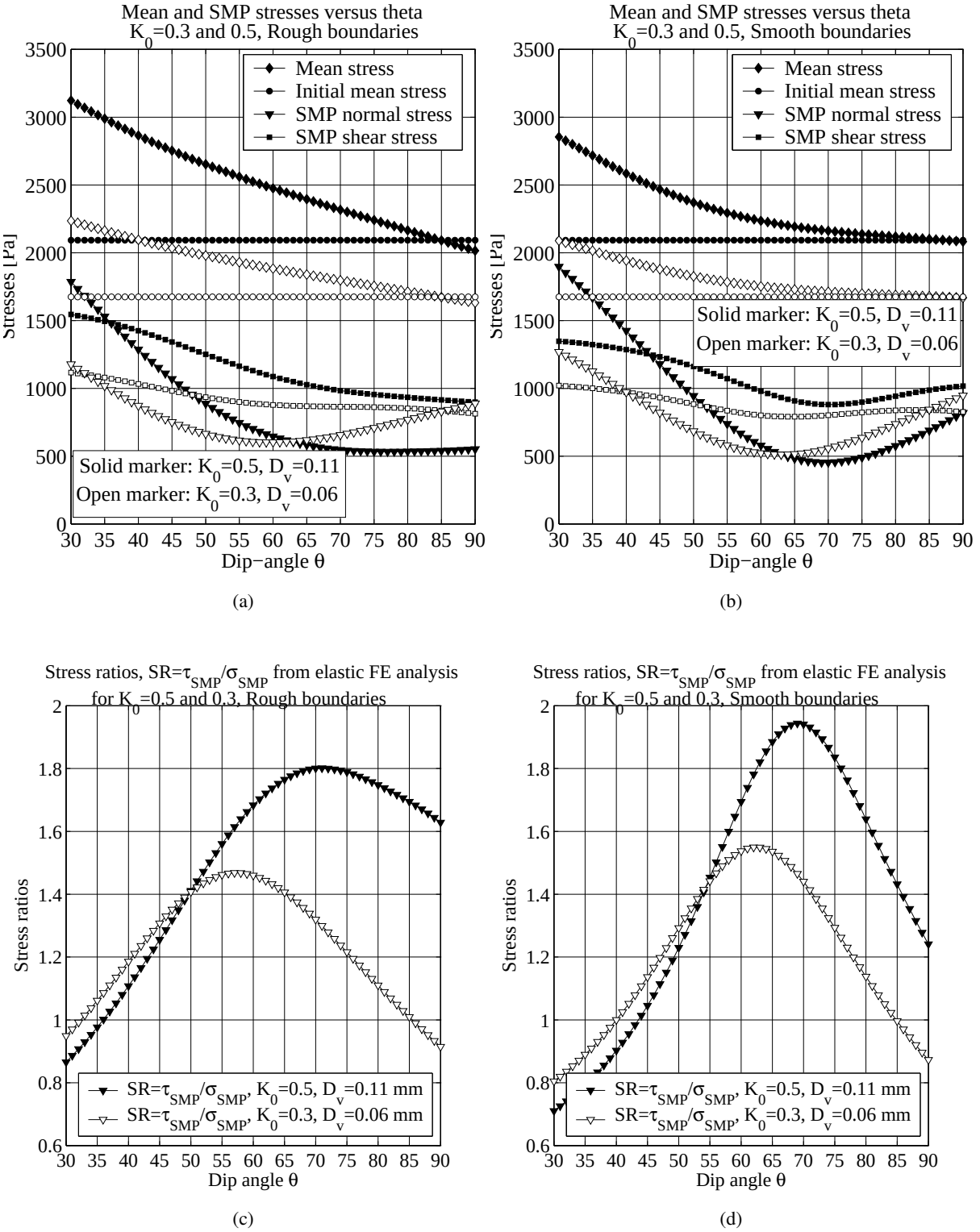

Figure 10: a) and b) Mean stress and stresses on spatial mobilize plane (SMP) and c) and d) stress ratio on SMP versus fault dip-angle θ.

to the stresses obtained from the FEM analysis. We then computed the stress state in the deposit as shown in Figure 9 at the intersection of the assumed fault rupture and mid-height line for a series of dip-angles between 30^{o}and 90^{o}. With the well-known generalized Mohr-Coulomb failure criterion (based on the so called Spatial Mobilized Plane,[24]) we computed the shear and normal stresses, the mobilized stress ratios, $\mathrm{SR}_{\mathrm{SMP}} = \tau_{\mathrm{SMP}}/\sigma_{normal,\mathrm{SMP}}$ for different dip-angles. Figures 10 a) and b) show stresses, and c) and d) stress ratios for different K_0 values and boundary conditions.

Results for both smooth and rough boundaries show increasing mean stresses (figures 10 a) and b)) as the dip-angles decreases since all dip-angles have the same vertical base offset but an increasing horizontal base offset with decreasing dip-angle (as to keep the $\mathrm{D_R}/\mathrm{L_R}$ constant). Figures 10 c) and d) show that all tress ratios have peaks between 57^{o} and 69^{o}, thus failure occurs first at these peaks; This does not seem to explain the reason why the most amount of uplift is needed for 60^{o} dip-angle. Returning to figures 10 a) and b) we see that the normal stresses on the spatial mobilized plane (SMP) all have minima between 60^{o} and 70^{o} dip-angles, except for rough boundaries and $\mathrm{K}_0 = 0.5$ (line with solid triangles in Figure 10 a)). Thus looking at this as progressive failure problem in which the shear band development length is important we conclude that the lower normal stresses on the SMP leads to a lower stress drop, $\Delta\tau_{\mathrm{SMP}} = \sigma_{\mathrm{SMP}}(\tan\phi_{\mathrm{peak}} - \tan\phi_{\mathrm{residual}})$ on the SMP.

Figure 11 shows stresses and stress ratios for two different uplifts with $\mathrm{K}_0 = 0.3$. The stress ratios (Figure 11b)) increases as expected due to the increasing deformation, but both the normal stress and shear stress decreases for increasing deformation. The shear stress decreases less than the normal stress leading to increasing stress ratio. Thus as deformation increases the stress drop decreases and assumingly also the shear band development length

Thus with these simple elastic analyses we seem to be able to explain the observations by Tani et. al.[13] that a larger uplift is necessary for dip-angles around 60^{o} (They have results for 45^{o}, 60^{o}and 75^{o} as seen in Figure 7).

More detailed numerical simulations with a constitutive law describing the non-linear soil behavior would be necessary for obtaining quantitative estimates of the required uplifts for a surface rupture, but the important point we have shown with the above analysis are:

1. Initial stress condition and the boundary conditions are of uttermost importance. Rigid boundaries as used commonly in experiments and most numerical models may only be appropriate if placed "far" away from the region of large shearing/rupture.

2. The mean pressure increases with increasing base offset for dip-angles <85^{o}

3. The normal stresses on the SMP decreases with increasing deformation.

These stress changes will affect the soil's stress-strain behavior which also affects the shear band development length. This will be elaborated on in the discussion section below.

(3) Inconsistent scale effects in 45^{o}dip-angle reverse fault

Lee et al.[15] results gives characteristic shear band development length (see Figure 6) independent (excluding some scatter) of the overburden stress for 45^{o} dip-angle reverse fault model experiment at both 1-g and centrifuge conditions. Seemingly there is no scale effect for 45^{o} dip-angle reverse faults. Ueta and Tani,[14] on the other hand, have obtained results that indicate that also for 45^{o} dip-angle reverse faults there is a scale effect, but to a lesser extent than in their 90^{o} dip-angle fault experiments.

To explain quantitatively the above inconsistent result is difficult without further knowledge of not only the initial stress conditions in the experiments, but also the stress-strain behavior of a soil subjected a simultaneous increase in shear deformation (base uplift) and increasing confining pressure (horizontal compression) as is the case in these 45^{o} dip-angle reverse fault model experiments.

Another important parameter of the above experiment is the aspect ratio of the model box. In Ueta and Tani's experiment the box was 1.55 meter long (for deposit heights < 0.5 meter) and the box of Lee et. al. was 3.0 meter long. The length of the box was held fixed for the different deposit

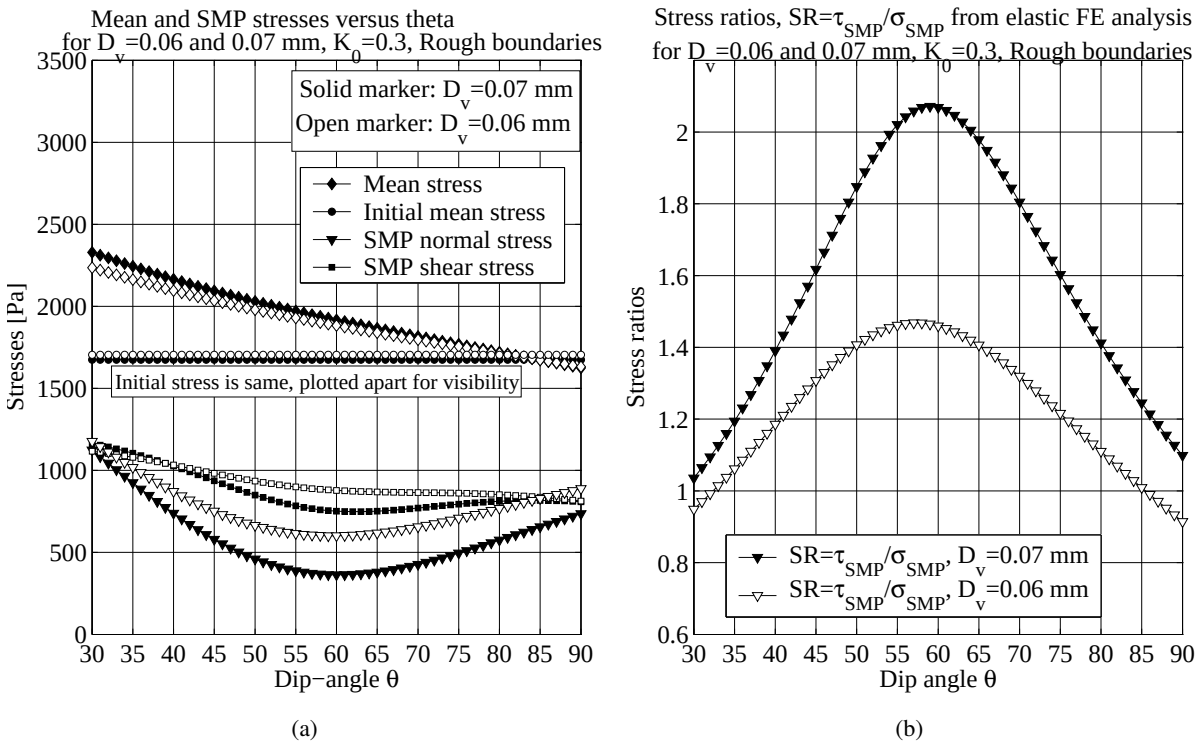

Figure 11: a) Mean stress and stresses on spatial mobilize plane (SMP) and b) stress ratio on SMP versus fault dip-angle θ for $\mathrm{K_0} = 0.3$ and vertical uplifts, $\mathrm{D_v}$, 0.06 and 0.07 mm.

heights. For two deposits with the same vertical uplift to height ratio, $\mathrm{D_v/H}$, the horizontal displacement is larger for the deposit with larger height, H, but it it has the same width as the smaller the deposit. Therefore the horizontal normal strains becomes larger for the larger deposit.

(4) Grain size effect on the shear band development length

Stone and Wood[12] have shown that similar vertical uplift to mean grain size ratio, $\mathrm{D_v/D_{50}}$, for sand with three different $\mathrm{D_{50}}$ gave similar deformation patterns in experiment with the same heights and widths for 90$^{\mathrm{o}}$ dip-angle dip-slip fault. The result shown in Figure 6 are based on these different amounts of uplift for the same deposit heights; Even though the stress conditions are thereby different, it seems the shear band development length increases with the grain size. This is expected since larger grain size of a sand, with otherwise similar grain characteristics, have larger dilatancy which results in a larger peak to residual stress drop.

The estimated characteristic shear band development lengths (105-314 $\mathrm{D_{50}}$) are on the order of the ones reported in[10,12] (100 $\mathrm{D_{50}}$and 176 $\mathrm{D_{50}}$). Though, discussing the shear band development lengths in terms of $\mathrm{D_{50}}$may not be appropriate since the stress conditions seem to have a big influence on the shear band development length.

(5) Vardoulakis et. al.

There is a large error margin shear band development lengths both due to our measurements and the variation of reported uplifts by Vardoulakis et. al.[9] We estimated shear band development length to approximately 2.5 cm or 76 $\mathrm{D_{50}}$, whereas Wood[5] estimates Vardoulakis et. al.'s length to 120 $\mathrm{D_{50}}$.

4. DISCUSSION

Here we comment on the above results; We will try to point out weak links in our argumentation and where more experiments and theoretical studies are needed.

(1) Peak to residual displacement along shear band, $\mathrm{D_{PR}}$

Is the peak to residual shear displacement, $\mathrm{D_{PR}}$, independent of element test specimen size and confining pressures? The relative displacement along the shear band, $\mathrm{D_{PR}}$was assumed independent of confining pressures as observed in biaxial tests at pressures of 78-400 kPa. Whether this is true for lower or higher pressures remains to verified.

More important, is whether the relative displacement along the shear band, $\mathrm{D_{PR}}$, is independent of the specimen size in element tests. If the shear band length (specimen width divided by cosine of shear band inclination, $\mathrm{W}/\cos(\theta)$) is much smaller (1 order of magnitude?) than the shear band development length, the assumption of shear band deforming in similar manner along its length may be valid. The peak to residual shear displacement's relation to stress conditions different from the ones in biaxial tests warrants further study.

(2) Parameters affecting stress drop

Larger confining pressure has seemingly two counter-acting effects on the stress drop, which in turn possibly affects the shear band development length. A larger normal pressure on the failure surface gives a larger stress drop. On the other hand a larger in confining pressure reduces soil dilatancy which decreases the stress drop.

Will the stress-strain curve for biaxial or triaxial test with simultaneous increasing load and confining pressure lead to smaller stress drop as hypothesized with question marks in Figure 12?

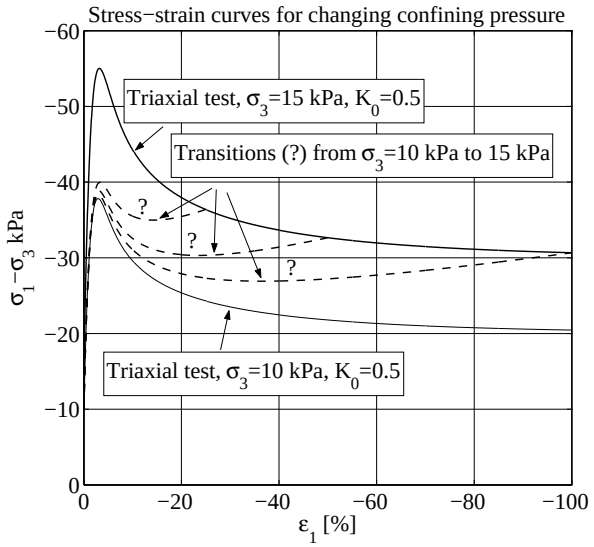

Figure 12: Stress strain curves for different confining pressures and hypothesized transitions from lower to higher confining pressure ($\sigma_3$varies from 10 to 15 kPa.)

Park and Tatsuoka[20] showed how the angle, δ, between the major principal stress direction and the bedding plane normal vector affects the peak friction angle and the overall stress-strain curve as shown in Figure 13. Thus inherent

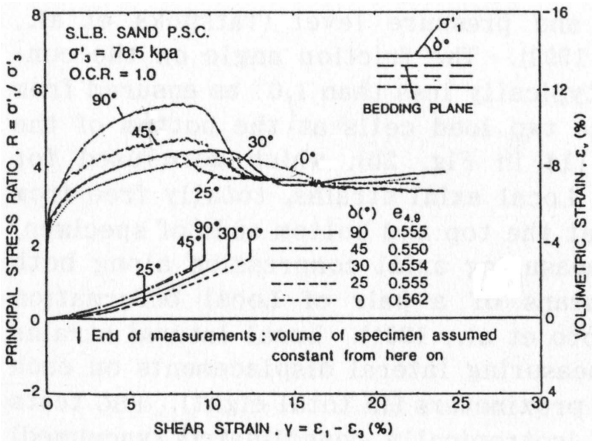

Figure 13: Stress-strain curves for plane strain compression test with varying angle between bedding plane normal and major principal stress axis (after Park and Tatsuoka.[20])

anisotropy changes the stress-strain behavior substantially with the largest stress drop is seen for angle, $\delta = 90^{\mathrm{o}}$ and for decreasing values of δ the stress drop is lower.

5. CONCLUSIONS

We have proposed a simplified method of estimating characteristic shear band development lengths, $\mathrm{L_d}$, by assuming it has one-to-one relation to the peak to residual shear displacement, $\mathrm{D_{PR}}$observed in biaxial tests. The method could prove useful when predicting shear band/rupture propagation through soils. The main points from the discussion above are:

- The peak to residual shear displacement, $\mathrm{D_{PR}}$ is independent of confining pressures in the 80-400 kPa range. Its dependency on other stress levels and loading conditions is unknown.
- The shear band development length seem to be closely related to the peak to residual stress drop, and therefore is affected by many factors, such as stress state, inherent anisotropy.
- For proper estimations of the peak to residual shear displacement, $\mathrm{D_{PR}}$ the element test specimen width should be smaller than the shear band development length.

Many further analytical and experimental studies are warranted to clarify above observations and we hope to address a few in a future publication.

ACKNOWLEDGMENT: We thank Professors Fumio Tatsuoka and Junichi Koseki for useful discussions. This research was supported by a part of the grant-in-aid No. 12355020 for scientific research (A) from the Japan Society for the Promotion of Science and is gratefully acknowledged. The first author also acknowledges the financial support in form a doctoral study scholarship by the Ministry of Education, Sports, and Culture of Japan.

References

1) Palmer, A. C. and Rice, J. R.: Growth of slip surfaces in progressive failure of over-consolidated clay, *Proceedings Royal Society London, A*, **332**, 527–548, 1973.

2) Vallejo, L.: Shear stress and hydraulic fracturing of earth dam soils., *Soils and Foundations*, **33**(3), 14–27, 1993.

3) Dégué, K., Soulié, M. and Ladanyi, B.: Extension of the griffith's fracture criteria to saturated clays, *International Journal for Numerical and Analytical Methods in Geomechanics*, **27**(4), 275–288, 2003.

4) Saada, A. S., Liang, L., Figueroa, J. L. and Cope, C. T.: Bifurcation and shear band propagation in sands, *Géotechnique*, **49**(3), 367–385, 1999.

5) Muir Wood, D.: Some observations of volumetric instabilities in soils, *International Journal of Solids and Structures*, **39**, 3429–3449, 2002.

6) Lade, P.: Analysis and prediction of shear banding under 3d conditions in granular materials, *Soils and Foundations*, **43**(4), 161–172, 2003.

7) Oie, N., M. Sato, Okuyama, Y., Yoshida, T., Yoshida, T., Yamada, S. and Tatsuoka, F.: Shear banding characteristics in plane strain compression of granular materials, Di Benedetto et. al., ed., *Proceedings of the 3rd International Symposium on Deformation Characteristics of Geomaterials, IS Lyon 03*, 597–606, Balkema, 2003.

8) Wang, X., Chan, D. and Morgenstern, N.: Kinematic modelling of shear band localization using discrete finite elements, *International Journal for Numerical and Analytical Methods in Geomechanics*, **27**(4), 289–324, 2003.

9) Vardoulakis, I., Graf, B. and Gudehus, G.: Trap-door problem with dry sand: a statical approach based upon model test kinematics., *International Journal for Numerical and Analytical Methods in Geomechanics*, **5**, 57–78, 1981.

10) Scarpelli, G. and Wood, D.: Experimental observations of shear band patterns in direct shear tests, Vermeer, P. and Luger, H., eds., *Deformation and Failure of Granular Materials, Proceedings IUTAM Symposium*, 473–484, Balkema, Rotterdam, 1982.

11) Lade, P. V. and Cole, D. A. J.: Multiple failure surfaces over dip-slip faults, *Journal of Geotechnical Engineering*, **110**(5), 616–627, 1984.

12) Stone, K. J. L. and Wood, D.: Effects of dilatancy and particle size observed in model tests on sand, *Soils and Foundations*, **32**(4), 43–57, 1992.

13) Tani, K., Ueta, K. and Onizuka, N.: Discussion on "Earthquake fault rupture propagation through soil" by J.D. Bray, R.B. Seed, L.S. Cluff and H.B.Seed, *Journal of Geotechnical Engineering, ASCE*, **122**(1), 80–82, 1996.

14) Ueta, K. and Tani, K.: Bedrock fault movements considering the accompanying deformation of quaternary deposits and ground surface, part 2 - normal and reverse fault model experiments, *Tech. Rep. U98048*, Central research institute of the electic power industry, CRIEPI, Denryokuchuokenkyuujou, 1999, (in japanese).

15) Lee, J. W., Hamada, M., Tabuchi, G. and Suzuki, K.: Prediction of fault rupture propagation based on physical model tests in sandy soil deposit, *Proceedings of the 13th World Conference on Earthquake Engineering, Paper No. 119*, International Association of Earthquake Engineering, 2004, published on CD-rom.

16) Bray, J. D., Seed, R. B., Cluff, L. S. and Seed, H. B.: Earthquake fault rupture propagation through soil, *Journal of Geotechnical Engineering*, **120**(3), 543–561, 1990.

17) Bishop: The influence of progressive failure on the choice of the method of stability analysis, *Géotechnique*, 168–172, 1971.

18) Puzrin, A. M. and Germanovich, L. N.: Shear band propagation in an infinite slope, *16th ASCE Engineering Mechanics Conference*, University of Washington, Seattle, 2003.

19) Yoshida, T. and Tatsuoka, F.: Deformation property of shear band in sand subjected to plane strain compression and its relation to particle characteristics, *Proceedings of the 14th international conference on soil mechanics and foundation engineering*, vol. 1, 237–240, 1997.

20) Park, C. S. and Tatsuoka, F.: Anisotropic strength and deformations of sands in plane strain compression, *Proceedings 13th International Conference on Soil Mechanics and Foundation Engineering*, vol. 1, 1–4, New Dehli, 1994.

21) Rudnicki, J. W. and Rice, J. R.: Conditions for the localization of deformation in pressure-sensitive dilatant materials, *Journal of the Mechanics and Physics of Solids*, **23**(6), 371–394, 1975, URL `http://www.sciencedirect.com/science/article/B6TXB-46G50H8-K2/2/dad922897ef1963e604902f26b074797`.

22) AnhDan, L. and Koseki, J.: Small strain behaviour of dense granular soils by true triaxial tests, (submitted to Soils and Foundations).

23) Sadr, A.: *Behavior of pile group embedded near surface fault rupture*, Ph.D. thesis, University of Tokyo, Japan, 2004, supervisor: Konagai, Kazuo.

24) Matsuoka, H. and Nakai, T.: Stress-strain relationship of soil based on the smp, *Proceedings of IX International Conference on Soil Mechanics and Foundation Engineering, Speciality Session 9*, 153–162, Tokyo, 1977.